

# UWB Channel Characteristics in the Proximity of a Dynamic Human Body for WBAN Medical Applications

Attaphongse Taparugssanagorn<sup>\*†</sup>, Carlos Pomalaza-Ráez<sup>\*</sup>,  
Raffaello Tesi<sup>\*</sup>, Matti Hämäläinen<sup>\*</sup>, Jari Iinatti<sup>\*</sup>, and Ryuji Kohno<sup>\*†</sup>

<sup>\*</sup>Centre for Wireless Communications, University of Oulu, Oulu, Finland

<sup>†</sup>Center of Medical Information & Communication Technology, Yokohama National University, Yokohama, Japan

**Abstract**—It is reasonable to assume that patients in hospitals and other medical facilities have various levels of mobility, e.g., walking, wheelchairs, eating, etc. There is also growing evidence that for most medical conditions having patients move or walk, as much as they can tolerate, will improve their health. Wireless body area networks (WBAN) are being considered as the enabling technology that will facilitate remote monitoring of patients' health status in such dynamic scenarios. The human body has a complex shape and consists of different tissues. It is then expected that the propagation of the electromagnetic waves, in WBANs, will have different characteristics than the ones found in other situations, e.g. outdoors, offices, etc. The contribution of the work described in this paper is to expand the knowledge of the ultra-wideband (UWB) channel in the frequency range of 3.1-10 GHz in close proximity of a dynamic human body. The experimental measurements are used to develop mathematical models for the radio channel. These models can then be used to better design communication network protocols for WBANs.

## I. INTRODUCTION

Wireless medical telemetry has been experiencing continuous developments and improvements during recent years [1]. In this type of application a patient's health is remotely monitored through the use of radio technology. As a result of this technology the number of medical devices that are physically connected to patients is minimized increasing their level of comfort and mobility. For the case of medical applications these devices are connected to sensors that monitor vital body parameters or movements. Ultra-wideband (UWB) communications has become a promising technology for WBANs due to its particular characteristics [2, 3]. The monitoring of human vitals and movements requires a relatively low data rate which in the case of UWB translates into very small transmitting power requirements, i.e., longer battery life. This is a very desirable feature for devices that are going to be close to the body and meant to be used for extended periods of time.

To design and develop UWB systems that will be used in WBAN applications it is necessary to measure, and then model, the corresponding radio propagation channel. For the case of indoor and outdoor scenarios comprehensive studies of the UWB propagation channel have been performed in recent years [2, 4, 5]. It is natural to expect that the channel characteristics for those cases will be different from the ones found in WBAN scenarios due to the effect of the human body with its complex shape and different tissues, each with a different permittivity [6]. UWB measurements around the human body have been carried out by various researchers [7-9]. However, no medical or technical reason has been given to justify those scenarios, e.g., using numerous antennas/transceivers very close to the human skin [8]. Experimental measurements under conditions more likely to be accepted in the medical care field were done in [10-11]. However, dynamic situations have not been covered in those studies. In this paper, we contribute to (a) experimental measurements under dynamic conditions, namely, body movements in scenarios which

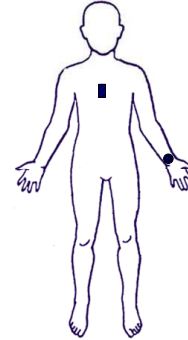


Fig. 1. Antenna positions for the 1<sup>st</sup> set of measurements. The rectangle represents the Rx antenna and the circle represents the Tx antenna.

most likely take place in the medical care field and (b) the analysis of these measurements and the development of appropriate UWB channel mathematical models. The scenarios under consideration include the radio links between sensor nodes themselves and between a sensor node to an UWB control node or gateway few meters from the body, e.g., on a wall or the ceiling as shown in [10-11].

The experiments were first conducted in an anechoic chamber. Measurements were taken for both static and dynamic situations. These results highlight the importance to carry out a comprehensive study of the nature of the propagation signals when they take place close to a human body. The effect of body motions is investigated and compared to the static situation. To obtain more realistic results the measurements were repeated in a regular hospital room. The measurements obtained in this study are used to estimate the channel parameters needed to build mathematical models that can be used in WBAN medical applications.

## II. CHANNEL MEASUREMENT SETUP AND SCENARIOS

The channel measurement system is the same as in [10-11] and consists of an HP Agilent 8720ES [12], a vector network analyzer (VNA), SkyCross SMT-3TO10M-A antennas [13], 5-m long SUCOFLEX<sup>®</sup> RF cables [14] with 7.96 dB loss and a control computer with LabVIEW<sup>™</sup> 7 software.

As a reference, the UWB channel measurement experiments were first conducted in an anechoic chamber to minimize other effects from the environment. The 1<sup>st</sup> set of measurements corresponds to the radio link between sensor nodes on the body (radio link A1). The Rx antenna is at the middle front of the torso and the Tx antenna is placed on the left wrist as shown in Fig. 1. These locations are comfortable for most patients and they are potential places for antennas/transceivers connected to electrocardiogram (ECG) sensors and a pulse oximeter. Considering that processing a single frequency

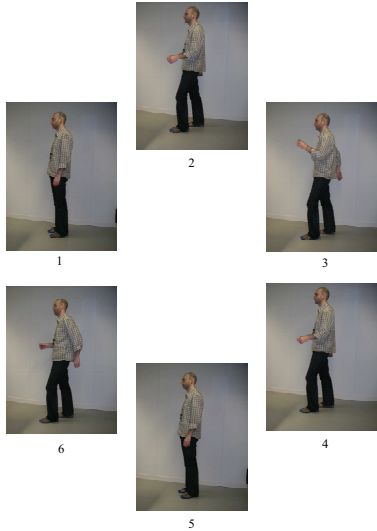


Fig. 2. Positions of a walking cycle.

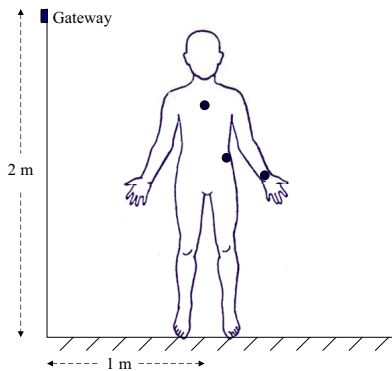


Fig. 3. Antenna positions for the 2<sup>nd</sup> set of measurements. The rectangle represents the Rx antenna and the circle represents the Tx antenna, respectively. There are three different directions for the Tx antenna: (1) facing the Rx antenna, (2) beside the Rx antenna, and (3) with the back towards the Rx antenna.

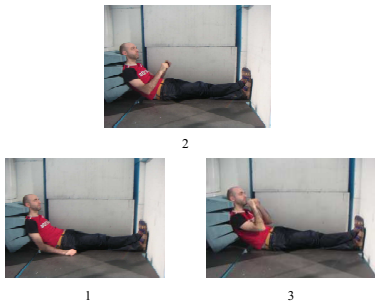


Fig. 4. Emulation of arm movements in a lying down position emulating, e.g., when having meals on the bed.

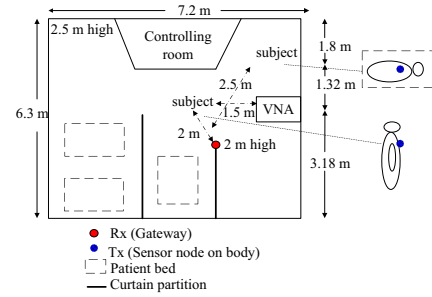


Fig. 5. Floor plan of a regular hospital room, where the 1<sup>st</sup> – 3<sup>rd</sup> sets of measurements were conducted.

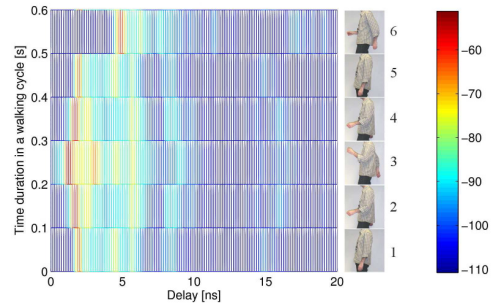


Fig. 6. Magnitude of the channel impulse response for each position in a walking cycle of the 1<sup>st</sup> set.

domain measurement in the 3.1-10 GHz band takes several seconds, a real-time measurement of the radio channel fluctuations due to body motions is not feasible. Instead, a pseudo-dynamic measurement method was applied, where each position in a walking cycle in Fig. 2 was kept still for the whole measurement period (e.g. 100 snapshots per position), and was modified according to the walking cycle.

Fig. 3 shows the positions for the 2<sup>nd</sup> set of measurements, with the Tx antenna at three different positions, i.e., the middle of the chest, the left-side of the waist, and on the left wrist. The Rx antenna is placed on a 2-m high wall. This emulates the radio link A2. A pseudo-dynamic measurement covering a walking cycle was again applied in this set of measurements. In addition, at each position of the Tx antenna, the measurements for different directions of the subject to the Rx antenna were conducted, i.e., (1) facing the antenna, (2) beside the antenna, and (3) with the back towards the antenna.

The 3<sup>rd</sup> set of measurements aims to investigate the situations when a patient is laying down and having a meal as illustrated in Fig. 4. We consider two cases of the radio links, i.e., A1 and A2. The first case (set 3.1) is when the Rx and the Tx antennas are placed at the middle front of the torso and on the left wrist of the subject, respectively. The second case (set 3.2) is when the Rx antenna is placed on a 2-m high wall, which is 1 m away from where the subject lays down. The Tx is placed at either the middle front of the torso or on the left wrist of the subject for the two subcases.

To obtain realistic results, all measurement sets were repeated in a regular hospital room with a size of 6.3 m×7.2 m×2.5 m as shown in Fig. 5.

### III. RESULTS AND ANALYSIS

One hundred different realizations of the channel impulse responses obtained from the inverse fast Fourier transform (IFFT) of the measured  $H(f)$  were averaged for each position. Since the energy

TABLE I  
RMS DELAY SPREAD  $\tau_{\text{RMS}}$  AND AMPLITUDE DISTRIBUTION OF THE STATIC AND PSEUDO-DYNAMIC MEASUREMENTS

Measurement scenario	RMS delay spread		Amplitude distribution	
	$\mu$ [ns]	$\sigma$ [ns]	Delay bin 1	Delay bin 5
<b>Set 1: static</b>	0.2087	0.0559	log-normal	log-normal
pseudo-dynamic	0.1371	0.0670	Weibull	Weibull
<b>Set 2.1: Tx at the left waist</b>	0.0839	0.0086	log-normal	log-normal
static: facing Rx	0.0998	0.0301	Weibull	log-normal
static: beside Rx	1.3332	0.2901	log-normal	log-normal
pseudo-dynamic: beside Rx	1.9282	1.0313	Weibull	log-normal
static: back towards to Rx	2.7254	0.6441	log-normal	Weibull
pseudo-dynamic: back towards to Rx	2.1163	1.2027	Weibull	Weibull
<b>Set 2.2: Tx at the left wrist</b>	0.0934	0.0251	log-normal	Weibull
static: facing Rx	0.1036	0.0576	Weibull	Weibull
static: beside Rx	0.0934	0.0251	log-normal	Weibull
pseudo-dynamic: beside Rx	0.1036	0.0576	Weibull	Weibull
static: back towards to Rx	0.1883	0.0774	log-normal	log-normal
pseudo-dynamic: back towards to Rx	0.5721	0.5959	Weibull	Weibull
<b>Set 2.3: Tx at the middle front of the torso</b>	0.0920	0.0222	Weibull	Weibull
static: facing Rx	0.1047	0.0290	Weibull	Weibull
static: beside Rx	0.3875	0.1725	log-normal	Weibull
pseudo-dynamic: beside Rx	0.2181	0.1952	Weibull	Weibull
static: back towards to Rx	0.7395	0.2033	log-normal	n/a
pseudo-dynamic: back towards to Rx	0.7867	0.2304	log-normal	n/a
<b>Set 3.1: Rx at the middle front of the torso</b>	0.0589	0.0008	log-normal	log-normal
static	0.0470	0.0695	Weibull	Weibull
pseudo-dynamic	0.0914	0.0058	log-normal	log-normal
<b>Set 3.2: Rx at a 2-m high wall</b>	0.1866	0.0961	Weibull	Weibull
static: Tx at the middle front of the torso	2.2935	0.5045	log-normal	log-normal
pseudo-dynamic: Tx at the left wrist	1.2115	1.5041	Weibull	Weibull

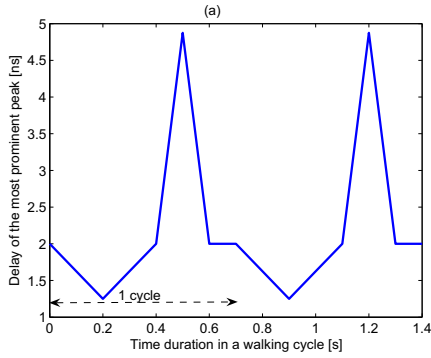


Fig. 7. Delay of the most prominent peak of the impulse response for each position in two walking cycles of the 1<sup>st</sup> set.

of these responses close to the human body decays rapidly we focus only on the first 20 ns of each channel impulse response. Fig. 6 shows the average of the magnitude of the channel impulse responses for each position in a walking cycle of the 1<sup>st</sup> set. As Fig. 6 shows, the arm motion during a walking cycle has a significant impact on the radio link from the Tx antenna on the left wrist to the Rx antenna at the middle front of the torso. For instance, when the left hand moves to the uppermost position 3, the strongest path arrives earlier than in the other positions due to the shorter distance between both antennas. There are also more significant paths due to the reflections of the wave out of the arm and the shoulder. The shadowing due to blocking of the body is noticed in position 6, where the left hand moves to the

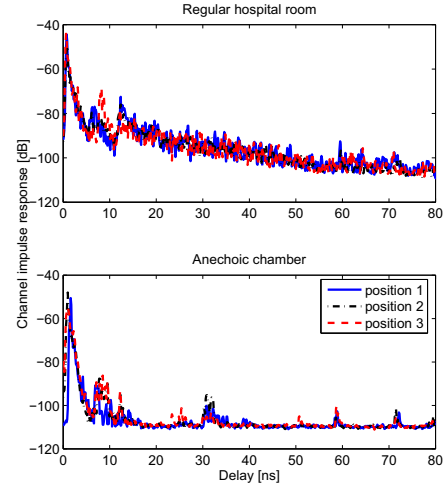


Fig. 8. Magnitude of the channel impulse response for each position in a eating cycle in the set 3.1

lowest position. Fig. 7 shows the delay of the most prominent peak of the impulse response for two walking cycles, respectively.

Fig. 8 shows the averaged channel impulse responses corresponding to each arm position in the measurement set 3.1. There is a larger delay for the first arriving wave and the reflecting waves in position 1 than in the other two positions since the Tx antenna is closer to the body and is farther from the Rx antenna. In addition, for position

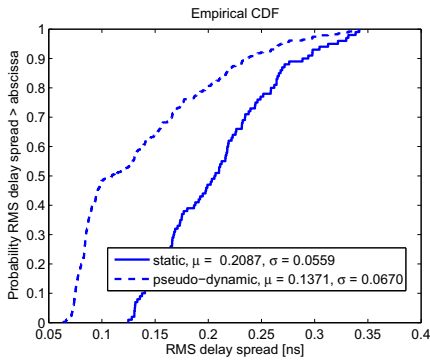


Fig. 9. RMS delay spread of the channel impulse response for each position in a walking cycle in the 1<sup>st</sup> set.

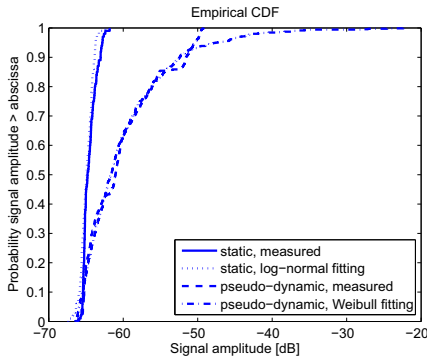


Fig. 10. Amplitude distribution of the first delay bin and the distribution fitting for static and pseudo-dynamic channels in the 1<sup>st</sup> set.

1 there is a larger antenna polarization mismatch than at the other positions.

To evaluate the delay dispersion within the channel a value of interest is the root mean square (RMS) delay spread  $\tau_{\text{RMS}}$ . To calculate it, all measured channel impulse responses are first truncated above the noise threshold set to four times of the noise standard deviation [15], i.e., -108.2 dB. The dynamic range varies depending on the different cases of the measurements. The mean  $\mu$  and standard deviation  $\sigma$  of the RMS delay spreads are summarized in Table I. The value of the RMS delay spreads depends on the probability of having shadowing due to blocking of the body and being at a closer distance between the Tx and the Rx antennas. For example, the result of 1<sup>st</sup> set of the measurements (Fig. 9) shows the static case has higher RMS delay spread than the pseudo-dynamic case. This is because the Tx antenna has higher probability to be closer to the Rx antenna. In addition, the standard deviations of the RMS delay spreads in the pseudo-dynamic cases are always larger than the ones in the static cases.

The Akaike information criterion (AIC), which calculates the discrepancy between a candidate model  $j$  ( $j = 1, 2, \dots, J$ ) with probability density function (pdf)  $g_j^j$  is applied in order to compare the distribution models against our empirical data [16]. Fig. 10 compares the amplitude distributions of the most prominent peak (first delay bin) and the distribution best fitting the static and pseudo-dynamic channels in the 1<sup>st</sup> set. We can see in Table I that the amplitudes of the first delay bin are log-normally distributed for most cases of the static situations. The Weibull distribution is the best one for characterizing the probabilistic nature of most of the amplitudes

of the first delay bin in the pseudo-dynamic situations. For the fifth delay bin, the amplitude distributions tend to be Weibull distributed for most cases. The last case of the measurement set 2.3, when the subject is back towards the Rx antenna, is marked as not available (n/a) since the signal level is too low to be of any use.

#### IV. CONCLUSIONS

We have conducted a series of UWB WBAN measurements in the frequency range of 3.1-10 GHz including the effect of body motions and constraints expected to be found in medical applications. The fluctuations of the radio channels under such dynamic situations can cause severe problems if not taken into account during a system design. A pseudo-dynamic measurement method was applied since a real-time measurement of the radio channel fluctuations due to the body motions is not technically feasible over a frequency band of several GHz. The differences of the results for both static and pseudo-dynamic situations were found in terms of the RMS delay spread and the amplitude distribution.

#### REFERENCES

- [1] H. S. Ng, M. L. Sim, C. M. Tan and C. C. Wong, "Wireless technologies for telemedicine," *BT Technology Journal*, Springer, vol. 24, no. 2, pp. 130-137, April 2006.
- [2] R. J. Cramer, R. A. Scholtz and M. Z. Win, "An Evaluation of the Ultra-Wideband Propagation Channel," *IEEE Trans. Antennas Propagation*, vol. 50, no. 5, pp. 561-570, May 2002.
- [3] S. Gezici and Z. Sahinoglu, "Theoretical Limits for Estimation of Vital Signal Parameters Using Impulse Radio UWB," *IEEE Communications Society subject matter experts for publication in the ICC 2007 proceedings*, 2007.
- [4] S. S. Ghassemzadeh and V. Tarokh, "The Ultra-Wideband Indoor Path Loss Model," Tech. Rep. P802.15 02/277r1SG3a, AT&T Labs, Florham Park, NJ, USA (IEEE P802.15 SG3a contribution, June 2002).
- [5] B. Kannan et al., "Characterization of UWB Channels: Large-Scale Parameters for Indoor and Outdoor Office Environment," IEEE P802.15 Working Group for Wireless Area Networks (WPANs) (IEEE 802.15-04-0383-00-04a, July 2004).
- [6] M. Klemm and G. Troester, "EM Energy Absorption in the Human Body Tissues due to UWB Antennas," in *Electromagnetics Research*, PIER 62, 261-280, 2006.
- [7] A. Alomainy, Y. Hao, Y. Yuan, and Y. Liu, "Modelling and Characterisation of Radio Propagation from Wireless Implants at Different Frequencies," in *Proc. European Conference on Wireless Technology*, Sep. 2006.
- [8] T. Zasowski, F. Althaus, M. Stäger, A. Wittneben, and G. Tröster, "UWB for Noninvasive Wireless Body Area Networks: Channel Measurements and Results," in *Proc. IEEE Conference on Ultra Wideband Systems and Technologies (UWBST)*, Nov. 2003.
- [9] A. Fort, C. Desset, J. Ryckaert, P. De Doncker, L. Van Biesen, and P. Wambacq, "Characterization of the Ultra Wideband Body Area Propagation Channel," in *Proc. International Conference ICU*, pp. 22-27, 2006.
- [10] A. Tapparugssanagorn, C. Pomalaza-Ráez, A. Isola, R. Tesi, M. Hämäläinen, and J. Iinatti, "UWB Channel Modelling for Wireless Body Area Networks in Medical Applications," in *Proc. International Symposium on Medical Information and Communication Technology (ISMICT)*, Feb. 2009.
- [11] A. Tapparugssanagorn, C. Pomalaza-Ráez, R. Tesi, M. Hämäläinen, and J. Iinatti, "Effect of Body Motion and the Type of Antenna on the Measured UWB Channel Characteristics in Medical Applications of Wireless Body Area Networks," in *IEEE International Conference on Ultra-Wideband (ICUWB)*, Sep. 2009.
- [12] <http://www.alliancetesteq.com/>.
- [13] <http://skycross.com/Products/PDFs/SMT-3TO10M-A.pdf>.
- [14] <http://www.hubersuhner.com>.
- [15] H. J. Zepernick and T. A. Wysocki, "Multipath channel parameters for the indoor radio at 2.4 GHz ISMband," in *IEEE Vehicular Technology conference*, vol. 1, pp. 190 - 193, July 1999.
- [16] U. G. Schuster, H. Bölcskei, and G. Durisi, "Ultra-wideband channel modeling on the basis of information-theoretic criteria," in *Proc. Int. Symp. Information Theory (ISIT)*, pp. 97-101, Sep. 2005.